Pluvial Flood Hazard Analysis in the Sub-catchment of the Metković City

Lovre Panđa[1,], Nino Krvavica[2], Ante Šiljeg[1], Fran Domazetović[1], Ivan Marić[1], Silvija Šiljeg[1], Rina Milošević[3]*

[1] University of Zadar, Department of Geography, Center for Geospatial Technologies, Zadar, Croatia, lpanda@unizd.hr; asiljeg@unizd.hr; fdomazeto@unizd.hr; imaric1@unizd.hr; ssiljeg@unizd.hr
[2] University of Rijeka, Faculty of Civil Engineering, Rijeka, Croatia, nino.krvavica@uniri.hr
[3] University of Zadar, Department of Ecology, Agronomy and Aquaculture, Center for Geospatial Technologies, Zadar, Croatia, rmilosevi@unizd.hr
* corresponding author

doi: 10.5281/zenodo.11643586

Abstract: Urban pluvial floods are a significant natural threat worldwide. In recent decades, their frequency and impact have been increasing primarily due to the combined effects of climate change, urbanization, and inadequate infrastructure. These floods result from intense rainfall overwhelming drainage systems. The research focuses on a specific 1.64 km^2 sub-catchment in Metković, chosen for its unique geographical, climatological, and ecological characteristics. Meteorological data spanning 1961-2020 from the Ploče station were utilized to analyse rainfall, producing hyetographs defining synthetic rainfall for various return periods. High-resolution spatial data, gathered using aeroLiDAR technology, facilitated the creation of digital surface (DSM) and terrain models (DTM). Additional data collection involved unmanned aerial vehicle (UAV) systems and a multispectral camera to generate a model with ten spectral bands. A hybrid approach combining Geographic Object-Based Image Analysis (GEOBIA) and manual correction was employed to develop a land cover and land use (LULC) model. This model, alongside infiltration, roughness, and imperviousness models derived from it, served as input data for pluvial flood hazard analyses. These analyses, conducted according to the methodology proposed within the Interreg STREAM project, involved hydrological-hydraulic simulations using HEC-RAS software. The outcomes comprise maps depicting water depth, velocity, and hazard levels corresponding to different probabilities. The research contributes to understanding and mitigating the risks associated with urban pluvial floods.

Keywords: urban pluvial floods; flood hazard; very-high resolution models.

1 Introduction

Floods are considered one of the greatest threats to humanity, leading to loss of life, damage to infrastructure, and significant economic losses (Singh et al. 2018). Climate change, intensive exploitation of natural resources, and improper land use have altered the hydrological response of catchments. These factors increase the frequency and severity of flood events. Furthermore, the combination of exposed, vulnerable, and inadequately prepared populations can exacerbate such situations and even generate additional risks. Insufficient capacities of authorities and public rescue services in these situations further increase the risk posed by major flood events (UNDRR 2010, Chaumillon et al. 2017). The rapid population growth in urban areas increases exposure to floods, and the risk is compounded by uneven social vulnerability, inadequate infiltration, and increased surface water runoff (Ochoa Rodriguez et al. 2012, de Moel et al. 2015). Therefore, flood prevention and mitigation in urban areas are recognized as international priorities that include flood hazard and risk assessments and the preparation of effective flood mitigation measures (WMO 2010). Although historically, fluvial floods have been the most documented, pluvial floods in urban areas have had the highest frequency share since 2000 compared to other types of floods in the same period (WGF 2016). Modeling flood hazards is a crucial part of flood risk assessment, risk management planning, and flood protection measures. Therefore, the main objective of this study is to conduct an analysis of pluvial flood hazards based on very high-resolution (VHR) spatial data collected using modern geospatial technologies.

2 Materials and methods

The research focuses on a specific 1.64 km^2 sub-catchment in Metković, chosen for its unique geographical, climatological, and ecological characteristics (Figure 1). Pluvial flood hazard analyses in the Metković sub-catchment were carried out following the methodology proposed and elaborated within the Study of flood hazard and risk assessment due to heavy rainfall and sea action in pilot areas in Croatia (Interreg STREAM 2023).

The methodological framework can be divided into several steps: 1) collection and processing of meteorological data; 2) collection and processing of aeroLiDAR data; 3) collection and processing of multispectral data; 4) Creation of VHR LULC and derivation of infiltration, roughness, and imperviousness models; 5) pluvial flood hazard analysis.

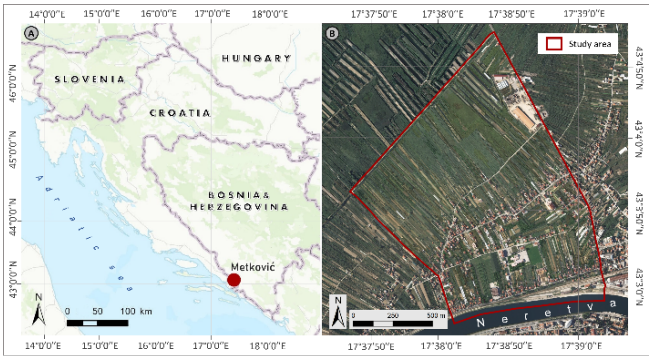

Figure 1. Geographical position of the study area: (A) In Croatia; (B) In Metković.

2.1 Collection and processing of meteorological data

The methodology for generating the design storm in Croatia has been presented in previous studies and scientific papers (Krvavica et al. 2018, Krvavica and Rubinić 2020), and further elaborated and improved within the framework of the Interreg project STREAM. Meteorological data spanning 1961-2020 from the Ploče station were utilized to analyse rainfall, producing hyetographs defining synthetic rainfall for various return periods. The generation of the design storm was carried out in three steps. Firstly, the identification and extraction of relevant storms from a series of measured pluviograph data were performed. Next, a dimensionless form of the design storm was defined for various durations. Finally, the design storm was generated for different durations and probabilities of occurrence.

2.2 Collection and processing of aeroLiDAR data

The aeroLiDAR survey utilized the UAV DJI Matrice M300 RTK along with the DJI Zenmuse L1 LiDAR payload. The survey mission was scheduled for 68 minutes, with a ground-sampling distance (GSD) of 2.73 cm/pix and a point-cloud density of 141 pts/m^2. The flight altitude was set at 100 m with a speed of 10 m/s, and the sensor's side overlap was set to 20%. Direct georeferencing was employed during data collection, with pre-flight calibration of devices to ensure accuracy. The LiDAR model's accuracy was evaluated using 229 checkpoints (CPs) collected by the RTK GNSS Trimble R12i. The reference points were compared with the collected point cloud and the RMSE was calculated. The acquired point cloud was processed using DJI Terra and Spatix softwares, with output in *.las* format. Data processing involved the exclusion of anthropogenic objects and vegetation, followed by five steps of data harmonization, including grouping point clouds based on recorded profiles, reducing inconsistencies across profiles, removal of intersecting points, smoothing, and thinning or removing inactive points. The resulting model was DTM, a basic spatial layer in hydrological-hydraulic simulations.

2.3 Collection and processing of multispectral data

A UAV Trinity F90+ equipped with a dual multispectral camera system (MicaSense RedEdge-MX Dual MS) was deployed for the multispectral survey. Data collection utilized the direct georeferencing method, incorporating global navigation satellite system (GNSS) and inertial measurement unit (IMU) data to accurately position the sensor platform during data acquisition. A total of nine CPs were acquired using the RTK GNSS Trimble R12i to assess the accuracy of the georeferencing system, as well as a base point (BP) for the UAV's iBase base station. UAV missions were planned with QBase 3D software, considering terrain morphology, desired detail levels, and flight duration. For multispectral imaging, front and side overlaps of 75% and 70% were selected, respectively, with a flight altitude of 120 m resulting in a GSD of 8.33 cm/px. Pre-flight calibration included the UAV's IMU and compass, along with radiometric calibration of the multispectral sensor using a reference panel, CRP2. The aerial photogrammetry process commenced post-calibration, accounting for atmospheric variations by repeating radiometric calibration after each mission. Geocoding of images primarily relied on UAV's flylog records and base station data, followed by processing using Agisoft Metashape software. This software facilitated the generation of a VHR 3D model through well-defined settings and steps, including photo orientation, dense point cloud derivation, deep filtering, and sensor location optimization. The resulting model was exported as UAV_{MS}.

2.4 Creation of VHR LULC and derivation of infiltration, roughness, and imperviousness models

The first step in the process of the pluvial flood hazard analysis was the derivation of VHR models (infiltration, roughness, and imperviousness) which are very important spatial layers for the accurate hydrological-hydraulic simulations in HEC-RAS software. To derive these three models, a VHR Land Use/Land Cover (LULC) model must be created. The development of the LULC model employed a hybrid method that combined GEOBIA (Blaschke 2010) with manual refinement techniques (MacFaden et al. 2012). This methodology encompassed several steps. Initially, UAV_{MS} image segmentation was conducted, where optimal parameter values for spectral and spatial details, as well as minimum segment size, were selected through an iterative process (n=25). Subsequently, in the second step, training samples were added using a probabilistic method of systematic sampling. The third step involved image classification using both Maximum Likelihood Classifier (MLC) and Support Vector Machine (SVM) algorithms. In the fourth step, accuracy assessment was performed using metrics such as Overall Accuracy (OA) and the Kappa Coefficient (KC) to determine the more accurate model between MLC and SVM. The fifth step entailed enhancing the quality of the LULC through manual interventions. The sixth step involved the derivation of infiltration, roughness, and imperviousness models by assigning specific values to LULC classes. For the infiltration model, a Curve Number (CN) was assigned to each LULC class based on the hydrological soil group according to the NRCS methodology (Hoeft 2020). For the roughness model, Manning's roughness coefficient (n) was added to the classes (Alizadeh and Berton 2023), while for the imperviousness model, LULC was reclassified into impermeable surfaces (such as buildings, greenhouses, asphalt, and water bodies) and permeable surfaces (various classes of vegetation etc.) (Šiljeg et al. 2023).

2.5 Pluvial flood hazard analysis

The flood hazard analysis was conducted for floods of small, medium, and large probabilities, with these probabilities being associated with the return period (5, 25, 100 years). The flood hazard analysis is based on hydrological-hydraulic simulations of surface runoff from heavy rainfall in HEC-RAS 6.0 software (Brunner 2021). The mathematical model of surface runoff from heavy rainfall consists of the following steps: 1) Defining the DTM; 2) Defining spatial parameters of infiltration processes; 3) Defining spatial density of built-up areas (impermeability);

4) Defining spatial distribution of roughness; 5) Defining spatial domain of the model and generating computational network; 6) Defining boundary conditions; 7) Defining numerical calculation parameters; 8) Defining scenarios. All spatial layers, including DTM, infiltration, roughness, and imperviousness models, are directly implemented into the HEC-RAS. The spatial model domain corresponds to the catchment area. The computational network is defined within the model domain, using a structured hexagonal grid with a width of 5.0 m. Three boundary conditions are defined in the model, two at the domain boundaries (line boundary conditions) and one across the entire domain surface (surface boundary condition): 1) At the land boundary of the domain, a condition of normal flow with average terrain slope is specified; 2) At the "river" boundary of the domain, a high sea level is specified (+0.5 m above mean sea level); 3) Across the domain surface, a spatially homogeneous but time-variable rainfall is defined in the form of a hyetograph (design storm). For numerical analysis of water flow, an unsteady 2D calculation was used along with the Diffusion Wave method with a time-variable time step. For the implicit calculation, the parameter $\theta = 1.0$ was used, and the PARDISO algorithm was used to solve matrices (Brunner 2021). The time step is dynamically calculated based on the CFL number ranging from 0.8 to 4.0. An analysis of three scenarios (5, 25, and 100 years) was conducted, and for each scenario, five calculations were performed for rainfall durations of 1, 3, 6, 12, 24 hours.

3 Results

The result of the rainfall analysis yielded synthetic rainfall durations for three probabilities (return periods of 5, 25, and 100 years), represented by rainfall intensity profiles known as rainfall hyetographs.

These hyetographs were generated to represent different durations and probabilities of occurrence, as illustrated in Figure 2A. After processing LiDAR data in DJI Terra, a DSM was generated (Figure 2B). Subsequently, a VHR DTM was created (Figure 2E) using Spatix software. The LiDAR model's accuracy resulted in an RMSE value of 0.0387 m, indicating a high level of accuracy. Despite the potential for higher spatial resolution in the DTM, the processing complexity necessitated exporting the model at a spatial resolution of 0.5 m. This DTM served as the basic spatial layer for the hydrological-hydraulic analyses. The UAV_{MS} model, with a spatial resolution of 0.08 m, comprised 10 spectral bands (Figure 2C). The UAV_{MS} model's accuracy was assessed using nine collected CPs, resulting in an RMSE of 0.0336 m. The UAV_{MS} model was used to generate the VHR LULC model. Through visual interpretation, specific parameters for the GEOBIA segmentation process were selected (spectral detail (20), spatial detail (19) and minimum segment size (15)), resulting in SVM and MLC classification models. A total of 6489 samples were added across 19 classes. The SVM algorithm demonstrated higher accuracy in classification and was improved by manual corrections (Figure 2D). By reclassifying the SVM LULC model and assigning values for CN, n, and 0 or 1, infiltration (Figure 2F), roughness (Figure 2G), and imperviousness (Figure 2H) models were generated. The simulation results presented the temporal dynamics of surface runoff, depicted as maximum recorded water depths and velocities. Finally, the outcome was depicted as models illustrating the maximum values of all parameters for each scenario. Figure 3 shows the depth (A) and velocity (B) of water, as well as the overall flood hazard level (C) for low-probability floods (100 years).

The subject sub-catchment has very low elevation differences and is predominantly flat, with a slight slope from the Neretva River embankment to the Jerkovac embankment, which defines the main direction of surface runoff. The greatest water depths occur in undeveloped areas between roads. Water velocities are very low due to gentle terrain slopes, with the highest levels of danger occurring in areas with the greatest water depths.

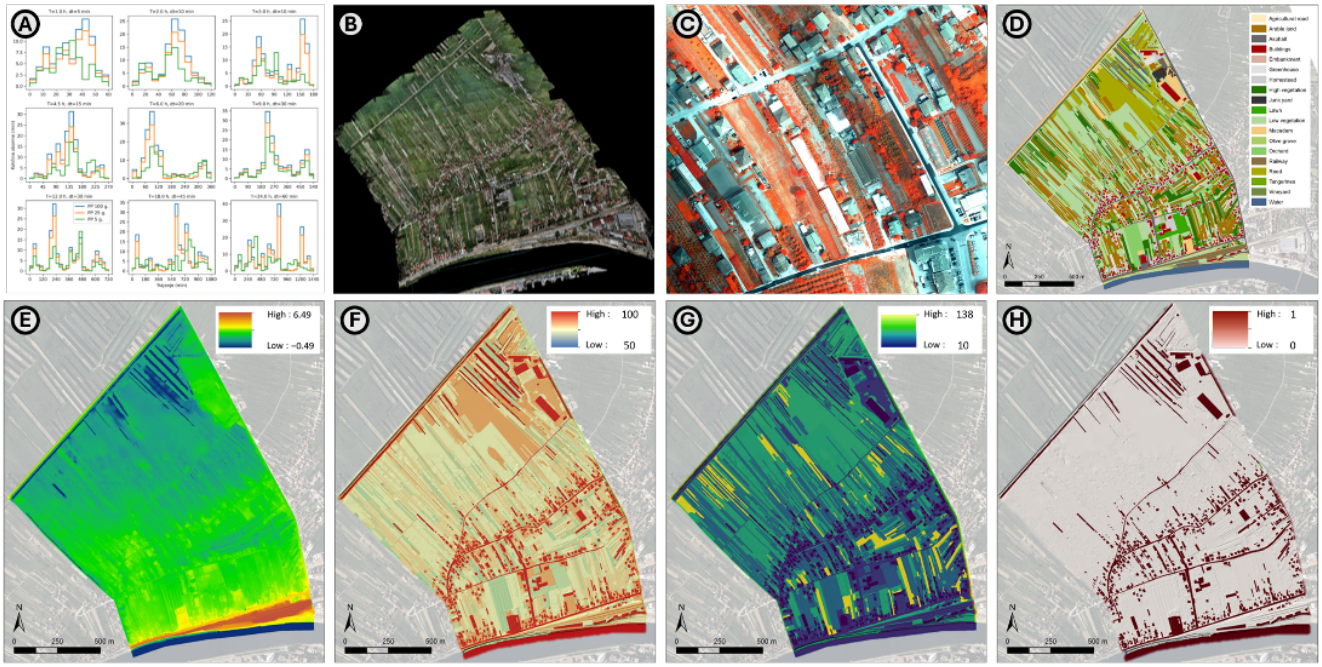

Figure 2. (A) Rainfall hyetographs; (B) DSM; (C) UAVMS; (D) LULC; (E) DTM; (F) Infiltration; (G) Roughness; (H) Imperviousness.

4 Discussion

Numerous user-defined parameters in the processes of data collection (UAV and multispectral camera calibration, flight altitude, flight speed, flight mission type, front and side overlap, etc.), processing (software, filtering data process, classification algorithms, number of LULC classes, number of samples, etc.), and analysis (size and type of computational network, boundary conditions, numerical calculation parameters, calculation method, etc.) can influence the output results. Therefore, it is crucial to approach the research process carefully and thoroughly. The VHR LULC model serves as an extremely important input data for hydrological-hydraulic analyses.

The process of UAV_{MS} segmentation and selection of a suitable classification algorithm presents a challenge. Parameters such as spectral and spatial detail and minimum segment size align with previous research utilizing GEOBIA (Šiljeg et al. 2023). Extremely low accuracy assessment results of the LULC model are attributed to the large number of classes with similar spectral characteristics (Dihkan et al. 2013). To obtain a more accurate model, it is necessary to manually correct misclassified segments of UAV_{MS} (Qu et al. 2021). Such a corrected model can provide reliable information on land cover and land use, which can assist decision-makers and emergency services in flood situations. Hydrological-hydraulic analyses based on accurate DTM, and models of infiltration, roughness, and imperviousness derived from LULC can accurately depict water depths and velocities, thus indicating the level of risk from pluvial floods in different scenarios (Interreg STREAM 2023).

5 Conclusions

The occurrence of pluvial floods in the research area is significantly influenced by the terrain topography and hydrological conditions, as well as by the built drainage and flood defence system (channels and embankments). Urban flood analysis using higher resolution and more detailed data has resulted in significantly more precise and reliable flood hazard maps compared to previous analyses. For more accurate and reliable modelling of pluvial floods, the installation of several meteorological stations with automatic rain gauges uniformly distributed throughout the watershed is recommended to obtain a more accurate picture of the rainfall regime. Additionally, monitoring water levels in main channels would greatly facilitate future flood analyses and ensure more reliable flood mitigation measures. Flood hazard analyses in urban areas can be further enhanced by integrating wastewater drainage systems into a coupled 1D/2D hydraulic model to simulate combined surface flow and pipe flow. To accomplish this, a survey of the entire drainage system, including manholes and pipelines, is necessary.

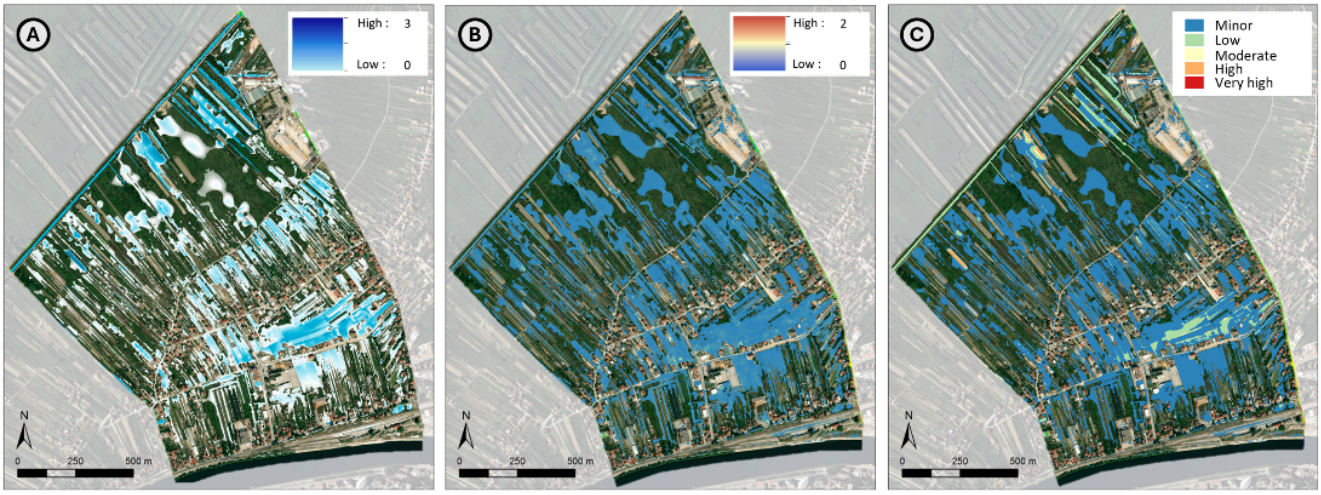

Figure 3. (A) Water depth; (B) Water velocity; (C) Flood hazard level.

6 References

Alizadeh, B., Rouzbeh B., 2023. CN-N: A Python-Based ArcGIS Tool for Generating SCS Curve Number and Manning's Roughness. Water 15 (20), 3581.

Blaschke, T., 2010. Object Based Image Analysis for Remote Sensing. ISPRS Journal of Photogrammetry and Remote Sensing 65 (1), 2-16.

Brunner, G.W., 2021. HEC-RAS 6.0 2D User's Manual.

Chaumillon, E., Bertin X., Fortunato, A.B., Bajo, M., Schneider, J.L., Dezileau, L., Walsh, J.P, Michelot, A., Chauveau, E., Créach, A., Hénaff, A., Sauzeau, T., Waeles, B., Gervais, B., Gwenaële J., Baumann, J., Breilh, J.F., Pedreros, R., 2017. Storm-Induced Marine Flooding: Lessons from a Multidisciplinary Approach. Earth-Science Reviews 165, 151-84.

De Moel, H., Jongman, B., Kreibich, H., Merz, B., Penning-Rowsell, E. Ward, P. J., 2015. Flood Risk Assessments at Different Spatial Scales. Mitigation and Adaptation Strategies for Global Change 20 (6), 865-890.

Dihkan, M., Guneroglu, N., Fevzi K., Guneroglu, A., 2013. Remote Sensing of Tea Plantations Using an SVM Classifier and Pattern-Based Accuracy Assessment Technique. International Journal of Remote Sensing 34 (23), 8549-8565.

Hoeft, C.C., 2020. Incorporating Updated Runoff Curve Number Technology into NRCS Directives. 78-87.

Interreg STREAM., 2023. Docs&Tools - STREAM - Italia-Croatia, https://programming14-20.italy-croatia.eu/web/stream/docs-and-tools. (Accessed 23 October, 2023)

Krvavica, N., Jaredić, K., Rubinić, J., 2018. Metodologija Definiranja Mjerodavne Oborine Za Dimenzioniranje Infiltracijskih Sustava. Građevinar 8.

Krvavica, N., Rubinić, J., 2020. Evaluation of Design Storms and Critical Rainfall Durations for Flood Prediction in Partially Urbanized Catchments. Water 12 (7).

MacFaden, S.W., O'Neil-Dunne, J.P.M., Royar, A.R., Lu, J.W.T., Rundle, A.G., 2012. High-Resolution Tree Canopy Mapping for New York City Using LIDAR and Object-Based Image Analysis. Journal of Applied Remote Sensing 6 (1), 063567.

Ochoa Rodriguez, S., ten Veldhuis, M.C., Maksimović, Č., Schertzer, D., Willems, P., 2012. Scientific Challenges for Enhancing Urban Pluvial Flood Resilience. in Geophysical Research Abstracts. Vol. 14. Copernicus GmbH.

Qu, L., Chen, Z., Li, M., Zhi, J., Wang, H., 2021. Accuracy Improvements to Pixel-Based and Object-Based Lulc Classification with Auxiliary Datasets from Google Earth Engine. Remote Sensing 13 (3), 453.

Singh, P., Sinha, V.S.P., Vijhani, A. Pahuja, N., 2018. Vulnerability Assessment of Urban Road Network from Urban Flood. International Journal of Disaster Risk Reduction 28, 237-250.

Šiljeg, A., Marinović, R., Domazetović, F., Jurišić, M., Marić, I., Panđa, L., Radočaj, D., Milošević, R., 2023. GEOBIA and Vegetation Indices in Extracting Olive Tree Canopies Based on Very High-Resolution UAV Multispectral Imagery. Applied Sciences 13 (2), 739.

Šiljeg, A., Panđa, L., Marinović, R., Krvavica, N., Domazetović, F., Jurišić, M., Radočaj, D., 2023. Infiltration Efficiency Index for GIS Analysis Using Very-High-Spatial-Resolution Data. Sustainability 15 (21), 15563.

UNDRR., 2010. Emerging Challenges for Early Warning Systems in Context of Climate Change and Urbanization, http://www.undrr.org/publication/emerging-challenges-early-warning-systems-context-climate-change-and-urbanization. (Accessed 10 April, 2024)

WGF., 2016. Pluvial Flooding: An EU Overview; European Commission and Water Group Floods (WGF), https://environment.ec.europa.eu/topics/water/floods_en. (Accessed 11 April, 2024)

WMO., 2010. PWS – 21: Guidelines on Early Warning Systems and Application of Nowcasting and Warning Operations (WMO/TD-No. 1559). https://library.wmo.int. (Accessed 11 April, 2024)